Effects of the Hawaiian Islands on the Vertical Structure of Low-level Clouds from CALIPSO Lidar

Jing-Wu Liu[1*], Shang-Ping Xie[2, 1], Su-Ping Zhang[1]

[1]Physical Oceanography Laboratory / Qingdao Collaborative Innovation Center of Marine Science and Technology, Key Laboratory of Ocean-Atmosphere Interaction and Climate in Universities of Shandong, Ocean University of China, Qingdao, China

[2]Scripps Institution of Oceanography, University of California San Diego, La Jolla, California

*Corresponding author: Jing-Wu Liu

Ocean University of China, 238 Songling Road, Qingdao, 266100, P. R. China

Email: liujingwu@126.com

Abstract

The steady northeast trade winds impinge on the Hawaiian Islands, producing prominent island wakes of multi-spatial scales from tens to thousands of kilometers. Cloud-Aerosol Lidar and Infrared Pathfinder Satellite Observations (CALIPSO) reveal rich three-dimensional structures of low-level clouds that are induced by the islands, distinct from the background environment. The cloud frequency peaks between 1.5-2.0 km in cloud-top elevation over the windward slopes of the islands of Kauai and Oahu due to orographic lifting and daytime island heating. In the nighttime near-island wake of Kauai, CALIPSO captures a striking cloud hole below 1.6 km as the cold advection from the island suppresses low-level clouds. The cyclonic eddy of the mechanical wake behind the island of Hawaii favors the formation of low-level clouds (below 2.5 km), and the anticyclonic eddy suppresses the low-level cloud formation, indicative of the dynamical effect on the vertical structure of low-level clouds. In the long Hawaiian wake due to air-sea interaction, low-level clouds form over both the warmer and colder waters, but the cloud tops are 400-600 m higher over the warm than the cold waters. In addition, the day-night differences and the sensitivity of low-level clouds to the background trade wind inversion height are also studied.

Key words: Hawaiian island wakes, low-level clouds, vertical structure, CALIPSO

1. Introduction

Low-level clouds have a strong effect on Earth's radiative budget for they effectively reflect incoming solar radiation with only a small influence on outgoing longwave radiation [*Wood*, 2012]. Because of their frequent presence over the ocean, low-level clouds have the largest cooling effect on the planet of all cloud types [*Hartmann et al.*, 1992]. However, since many of the physical processes controlling low-level clouds remain obscure, they are one of the prime contributors to the uncertainties of climate model projections [*Bony and Dufresne*, 2005; *Sherwood et al.*, 2014].

Under the descending branch of the Hadley circulation, low-level clouds are frequently observed over the subtropical North Pacific [*Norris*, 1998a, 1998b], where the steady northeasterly trade winds prevail throughout the year, especially in boreal summer [*Schroeder*, 1993]. The large-scale subsidence produces a thin but strong trade wind inversion (TWI) at 2500 m [*Cao et al.*, 2007; *Zhang et al.*, 2012]. Strong TWI confines convective activities and moist air beneath it, favoring the formation of stratus and stratocumulus clouds [*Norris*, 1998a]. Changes of atmospheric circulation and TWI alter the properties of low-level clouds [e.g. cloud height, thickness and occurrence; *Myers and Norris*, 2013].

Standing in the path of the northeasterly trade winds, the Hawaiian Islands modulate atmospheric circulation on multi-spatial scales from tens to thousands of kilometers, and thereby influence low-level clouds [*Smith and Grubišic*, 1993; *Xie et al.*, 2001; *Yang et al.*, 2008a, 2008b]. The cloud frequency increases significantly over the windward slopes of the Hawaiian Islands due to orographic lifting [*Yang and Chen*, 2008; *Yang et al.*, 2008a, 2008b]. Cloud bands trailing from west coasts of Kauai and Oahu downstream for less than 100 km are frequently observed in satellite images in the afternoon [*Yang et al.*, 2008b], as the daytime warm advection from the island lowers the sea surface pressure (SLP) and anchors a cloud band in the wake. At night, by contrast, the cold advection from the island suppresses the cloud formation. We refer to this warm/cold advection induced wake as the near-island wake.

While the near-island wakes trail just for tens of kilometers off Kauai and Oahu, the wake due to the direct hydrodynamic effect of the island orography extends 200 km downstream with two elongated counterrotating quasi-steady eddies behind the Big Island [*Smith and Grubišic*, 1993; hereafter the mechanical wake]. Individual mechanical wakes are visible in satellite images with cloud bands within the cyclonic eddy [*Smith and Grubišic*, 1993] and dissipate quickly downstream. A broad wake due to air-sea interaction takes their place 300 km downwind [*Xie et al.*, 2001; hereafter the ASI wake]. The wind curls induced by the Hawaiian Islands force oceanic Rossby waves and generate an eastward current that draws warm water from the west, causing a warm sea surface temperature (SST) tongue that anchors a cloud wake trailing westward for 3000 kilometers [*Xie et al.*, 2001].

Thus, the atmospheric response to the Hawaiian Islands is of multi-spatial scales. The vertical structure of low-level clouds holds the key to understanding the formation mechanisms of the island wakes. Previous studies generally focus on the presence of the cloud wakes using visible images and liquid water path (LWP) observed by satellite, but few studies examine the vertical structure of the cloud wakes with observational data. *Yang et al.* [2008a, 2008b] simulated the vertical development of near-island wakes for the islands of Hawaii and Kauai, respectively, which needs to be evaluated by observed data.

The Cloud–Aerosol Lidar and Infrared Pathfinder Satellite Observations (CALIPSO) satellite was launched on 28 April 2006 by the National Aeronautics and Space Administration (NASA) and the French Centre National d' Etudes Spatiales to study the impact of clouds and aerosols on Earth's radiation budget and climate [*Winker et al.*, 2009]. It provides a cloud-layer product according to the lidar backscatter strength with high spatial resolution up to 333 m along its tracks and 30 m in the vertical [*Vaughan et al.*, 2009]. Based upon CALIPSO, cloud vertical structures of small spatial scales have been studied [*Medeiros et al.*, 2010; *Stein et al.*, 2011; *Bouniol et al.*, 2012; *Liu et al.*, 2014]. Thus, CALIPSO offers the capability of revealing the vertical structure of low-level clouds in the Hawaiian Island wakes. *Zhang et al.* [2012] studied the cloud-base, cloud-top, and TWI base heights over the Hawaiian area using CALIPSO, and found that TWI modulates local precipitation by controlling the cloud thickness (TWI base height minus cloud-base height). They noticed the cloud thickness is smallest on the lee sides of Hawaiian Islands, but did not explicitly consider the effects of the islands and island wakes.

The present study investigates how low-level clouds respond to the multi-spatial scale island wakes of Hawaii with a focus on the vertical structure, by using CALIPSO in synergy with other high-resolution satellite observations, reanalysis and in situ soundings. Far away from any other landmass and standing in a steady trade wind regime, the Hawaiian Islands offer an ideal laboratory to study island perturbations. There the marine atmospheric boundary layer (MABL) is well separated by a strong TWI from the overlying free atmosphere. The mountains and diurnal heating of the islands induce rich patterns in circulation, cloud and rainfall in both the near and far fields. CALIPSO offers a unique view of the rich island effects from a cloud top perspective. To our knowledge, this is the first study examining the detailed vertical structure of low-level clouds in response to the mechanical and thermal forcing of the Hawaiian Islands. We show pronounced variations in cloud top height between the maintain slopes and lee ocean, and between day and night, in the near and far fields of the islands.

The rest of this paper is organized as follows. Section 2 introduces the datasets used in the present study. Section 3 describes the vertical structure of low-level clouds over the island and in the island wakes. Sections 4 and 5 investigate the day-night differences of low-level clouds and the sensitivity to the TWI height, respectively. Section 6 is a summary and discussion.

2. Data

We use a suite of high-resolution satellite observations, reanalysis, and radiosonde data to investigate how the Hawaiian Islands influence low-level clouds. Our focus is on boreal summer (May to October) when the northeasterly trade winds are steady [*Schroeder*, 1993] and TWI is strong [*Cao et al.*, 2007]. Since CALIPSO is available from June 2006, the present study covers the seven summers (May of 2007-13, June-October of 2006-12) when the Tropical Rainfall Measuring Mission (TRMM) Microwave Imager (TMI), ERA-Interim and soundings at Lihue and Hilo are also available. Although QuikSCAT do not overlap CALIPSO perfectly, we average QuikSCAT wind velocity for May to October 1999-2009 as summer climatology.

a. Satellite observations

We use the cloud layer product of CALIPSO with 333 m along-track resolution (http://www-calipso.larc.nasa.gov/; [*Winker et al.*, 2009]) to investigate low-level cloud structure over the Hawaiian region. Details on the retrieval algorithm can be found in *Vaughan et al.* [2009]. This product provides up to five cloud top heights below 8.5 km, and the minimal vertical distance between two cloud tops is 30 m. All cloud tops below 4 km are considered to be low-level cloud top (LCT). *Zhang et al.* [2012] interpreted the highest cloud top below 4 km as MABL height to study the spatial pattern of the MABL near the Hawaiian Islands. We include all cloud tops below 4 km to focus on the vertical distribution of low-level clouds. Although multi-layer clouds increase slightly the LCT frequency, the overall patterns are similar to those only with the highest cloud tops. Low-level clouds can be observed by CALIPSO only when optically thick higher-clouds are absent. It is not a problem for this study because low-level clouds are dominant near the Hawaiian Islands.

CALIPSO is sun-synchronous, passing over the same part of the Earth at roughly the same local time. CALIPSO observes the Hawaiian region around 2400 UTC (1400 HST) during the daytime and 1200 UTC (0200 HST) during the nighttime, and repeats its tracks every 16 days. By using CALIPSO observations near cross points between the daytime and nighttime tracks, we investigate the day-night differences in low-level clouds.

We use LWP observed by TMI available on Remote Sensing Systems (http://www.remss.com/; [*Hilburn and Wentz*, 2008]) on a 0.25° × 0.25° grid to construct a summer LWP climatology to track the horizontal pattern of the low-level cloud frequent following *Xie et al.* [2001]. We also use QuikSCAT winds on a 0.25° × 0.25° grid from Remote Sensing Systems to depict the large-scale background circulation in the Hawaiian region and small-scale surface wind pattern induced by the Hawaiian Islands. Based upon TMI LWP and QuikSCAT winds, *Xie et al.* [2001] detected an ASI wake trailing westward behind the Hawaiian Islands over 3000 kilometers. In addition, AVHRR SST (http://www.ncdc.noaa.gov/sst/; [*Reynolds et al.*, 2007]) on a 0.25° × 0.25° grid is averaged during the analysis period and spatially high-pass filtered to highlight the small-scale SST variations of the ASI wake.

b. Reanalysis data

We employ 6-hourly ERA-Interim fields on a 0.75° × 0.75° grid provided by the European Center for Medium-Range Weather Forecasts (ECWMF). ERA-Interim is the latest global atmospheric reanalysis. Substantial improvements in many aspects have been made for ERA-Interim comparing with ERA-40 [*Dee et al.*, 2011]. ERA-Interim uses National Centers for Environmental Prediction Real-Time Global SST on a 0.083° × 0.083° grid for January 2002-09 and Operational SST and Sea-Ice Analysis on a 0.05° ×

0.05° grid for February 2009 to present. The 6-hourly fields at 0000 and 1200 UTC are used in this study since they are close to the time CALIPSO passes the Hawaiian region. The horizontal resolution of ERA-Interim is high enough to depict the ASI wake, whose scale is about 500 kilometers in the meridional, but it is insufficient to resolve the atmospheric circulation in the mechanical and near-island wakes and over islands of scales less than 150 km.

c. Soundings

We employed atmospheric sounding data at Lihue (21.97°N, 159.33°W) on Kauai Island and at Hilo (19.72°N, 155.05°W) on the Big Island provided by the University Wyoming (http://weather.uwyo.edu/upperair/sounding.html) to investigate the sensitivity of LCT to the TWI height. Atmospheric soundings are available at 0000 and 1200 UTC times close to those of CALIPSO observations in the Hawaii region. The soundings at Hilo and Lihue typically have 12-14 vertical levels below 800 hPa, suitable for the climatological study of the structure of atmospheric boundary layer. *Cao et al.* [2007] used these soundings to investigate the temporal variations of TWI in Hawaiian trade wind regime.

3. Summer cloud distribution

In boreal summer (from May to October), the northeast trade winds are steady, and SST is between 24-27 °C in the Hawaii region (Figure 1a). The climatological surface winds are about 8 m s^{-1} and significantly weaken on the lee ocean of the islands, producing a westerly reverse flow in the broad wake of the island chain in the spatial high-pass filtered wind field (Figure 1b). As the ambient condition, the large-scale subsidence near Hawaii maintains a prominent TWI at 2.07 km in height in the annual mean according to *Zhang et al.* [2012].

LCT frequency (FQ) based upon CALIPSO observations is calculated as follow:

$$FQ = \frac{N_{LCT}}{N_{obs}} \times 100\%, \quad (1)$$

where N_{LCT} is the number of LCT within a 0.05° (lat) × 0.1 km (vertical) bin and N_{obs} is the total number of observations within the 0.05° lat bin. The daytime and nighttime CALIPSO tracks are indicated with black and blue lines in Figure 2, respectively. The tracks near the Hawaiian Islands are numbered with D1-4 (daytime) and N1-4 (nighttime). Figures 3 shows LCT frequencies along tracks D1, D2 and N1 between 15-25°N, respectively. In 22-25°N, the three tracks are located at least 200 km away from the Hawaiian Islands in the upstream environment where the trade winds are not disturbed. The undisturbed LCT frequency is almost featureless in space both during the daytime and nighttime. Most LCTs randomly fall into between 0.7 and 3.0 km in altitude, consistent with the results of *Cao et al.* [2007] based on the soundings at Lihue. They found that most TWIs are between 1.0 and 3.0 km. Figures 3b and 3c show that the Hawaiian Islands exert strong influences on low-level clouds as will be analyzed latter in this section. The LCT frequency between 19-20.2°N along track D1 reaches up to 8% between 1.6 and 2.1 km, which is much higher than that in the ambient condition and due to surface wind convergence on the windward side of the Big Island (Fig. 1). The vertical range of LCT is little broader during the nighttime than daytime, and low-level clouds are more frequent at night, indicative of diurnal variations of LCT that will be discussed in section 4.

a. Over islands and in near-island wakes

We employ the results of *Yang et al.* [2008a, 2008b] based upon MODIS and GOES superimpose CALIPSO tracks (Figure 4) to track the horizontal cloud patterns near Kauai and the Big Island. The time periods are June to August 2004-05 for MODIS cloud frequency (Figures 4a and 4c) and August 2005 for GOES brightness temperature

(Figures 4b and 4d), not perfectly overlapping the period of present study. The difference in analysis period is not a severe problem since the background circulation and MABL structure persist throughout the summer [*Cao et al.*, 2007].

CALIPSO passes the windward slope of Kauai along track D4 during the daytime (Figure 4a), and the island topography along the track is lower than 0.9 km (Figure 5a). Low-level clouds are much more prevalent over the windward slope than over the surrounding waters, consistent with the horizontal pattern of cloud fraction in JJA based on MODIS Aqua (Figure 4a). *Yang et al.* [2008b] found that the large cloud fraction over the windward slope persists from the late morning (around 1100HST) to early afternoon (around 1400 HST, their Figures 3a and 3b), and attributed it to orographic lifting of combined trade wind-anabatic flow and the daytime island heating. Our CALIPSO results suggest that the most LCTs are confined below 3.0 km (Figure 5a), close to the altitude of maximum MABL height in the Hawaiian region [*Cao et al.*, 2007]. The vertically integrated LCT frequency exceeds 80 % right above the windward slope, and decreases significantly to the south and north of Kauai Island (< 23 %), to the values even lower than the upstream environment (~30 %, not shown). This is because of the descent motion on the lee side induced by the topography effect, consistent with vertical velocity near Kauai simulated by *Yang et al.* [2008b].

CALIPSO also passes the windward slope of Oahu along track D3. The results are similar to Kauai, but the LCT response is weaker. The vertically integrated LCT frequency increases from 20 % over the waters near Oahu to 78 % over the windward slope. The contrast in low-level clouds between the windward slope and surrounding waters is weaker for Oahu than for Kauai, probably due to the lower elevation of Oahu (less than 0.5 km along the CALIPSO track).

At night, CALIPSO passes the lee ocean of Kauai at the nearest 2 km away from the west coast (Figure 4b). CALIPSO captures a striking “cloud hole” below 1.6 km in the lee. The nighttime LCT frequency off the island (south of 21.5 °N and north of 22.3 °N) is roughly 3-5 %, but it sharply decreases to less than 1 % in the cloud hole. *Yang et al.* [2008b] argued that the cold advection from Kauai during the nighttime is responsible for the cloud decrease. Because of the longwave radiation cooling at night, the land surface lowers the low-level temperature in the boundary layer. The trade winds advect the cold air from the island to the lee ocean, increasing SLP there. As a result, the downward motion induced by positive SLP anomalies suppresses the formation of low-level clouds. *Yang et al.* [2008b] found that the brightness temperature is 3-4 K higher over the lee waters than in the upstream environment, indicating reduced cloud occurrence in the near-island wake. The results based upon CALIPSO suggest that the cloud suppression by the nighttime cold advection only occurs below 1.6 km, which is close to the maximum elevation of Kauai. Above this level, the LCT frequency does not change much from the ambient. This supports *Yang et al.* [2008b]'s argument that the cold air from Kauai just increases the pressure below it. In addition, track N4 is in the shadow of Kauai, and the mountains may block advection of cloud water. A similar cloud hole occurs over the lee ocean of Oahu and Molokai (Figure 5d), suggesting that the nighttime cloud hole is prevalent over the lee ocean of the islands.

The daytime warm advection lowers the lee SLP and produces a 20-km long cloud band over the lee ocean of Kauai according to MODIS [*Yang et al.*, 2008b]. Unfortunately, CALIPSO does not pass these cloud bands of near-island wakes during the daytime, and therefore cannot depict their vertical structures.

With the maximum 4.2 km elevation, the Big Island is much taller than Oahu and Kauai, standing well above the TWI, splitting the northeast trade winds, and inducing a westerly reverse flow in the wake [*Smith and Grubišic*, 1993; *Yang et al.*, 2008a]. Two CALIPSO tracks (Figures 4c and 4d) pass the Big Island, mostly observing clouds over the leeside slope of the Big Island south of 20 °N. The LCT frequency reaches up to 9%

between 1.5 and 3.0 km over the lee side of the Big Island in the day, much higher than the surrounding waters (Figure 5e). The vertical structure of LCT frequency features three peaks, sandwiching two minima lee of Mauna Kea and Mauna Loa. These LCT peaks over the leeside slope are induced by orographic lifting by combined westerly return wind-anabatic flow and the daytime island heating [*Yang et al.*, 2008a]. The LCT is less frequent over the regions with topography higher than 2.0 km, possibly because the return flow is much shallower than the easterly trade winds. LCTs are frequent at or above 2.5 km, the upper limit of ambient LCT height, over the Big Island (Figure 5e), suggestive of the effects of land surface heating during the daytime.

CALIPSO observes the clouds over the windward slope and over the lee ocean of Kohala Mountains of the Big Island along tracks N1 and D2 during the nighttime and daytime between 20-20.5 °N (Figures 4c and 4d), respectively. There is a steep transition of LCT frequency from the windward slope to the lee ocean. The LCT frequency over the windward slope reaches up to 7% during nighttime, and decreases below 2% over the lee ocean. The vertically integrated LCT frequency along track N1 and D2 shows the contrast more clearly (black lines in Figures 5e and 5f). It reaches up to 60% over the windward slope, and is lower than 20% over the lee ocean. The former maximum of LCT frequency is due to daytime heating and the strong uprising motion induced by orographic lifting, which reaches 25 cm s^{-1} over the windward slope at according to the model simulation results of *Yang et al.* [2008b, their Figure 7e]. The latter LCT frequency minimum persists throughout the day [*Yang et al.*, 2008a] and is caused by the downdraft over the lee ocean in pair with the orographic updraft over the windward slope [*Smith and Grubišic*, 1993; *Yang and Chen*, 2003]. On the south slope of Mt. Loa (south of 19.2 °N), the LCT height slopes down rapidly, suggestive of a hydraulic jump [*Smith and Grubišic*, 1993]. The sloping down is most clear during the day but visible at night.

b. In the mechanical wake of the Big Island

Two elongated counterrotating quasi-steady eddies form over the lee waters of the Big Island that are induced by fluid mechanical effects of the island and extend over about 200 km to the west-southwest [*Smith and Grubišic*, 1993]. In climatology, the mechanical wake behind the Big Island features a pair of surface wind convergence and divergence bands, and therefore causes a pair of LWP maximum and minimum (Figure 2b). CALIPSO flies over this mechanical wake along tracks D3 and D4 during the daytime, and along N2 and N3 during the nighttime. The LCT, LWP and surface wind divergence along above four tracks are composited referenced to the latitudes of the mean LWP maximum (Figure 6). The surface wind convergence is much stronger (about $-3\times10^{-5}\ s^{-1}$) in the cyclonic eddy than the divergence in the anticyclonic eddy (about $1\times10^{-5}\ s^{-1}$). LWP is correlated with surface wind convergence, suggesting that the mechanical wake of the Big Island produces a pronounced cloud wake. CALIPSO captures this cloud wake with LCT frequency maximum (upper panel in Figure 6) collocated with the convergence and LWP maximum. Over the anticyclonic eddy, low-level clouds are less frequent in 1.0-1.5° south relative to the LWP maximum.

c. In the ASI wake

The wind curls induced by the Hawaiian Islands force oceanic Rossby waves, producing an eastward current that advects warmer water from the west *Xie et al.* [2001]. The resultant warm SST tongue modulates wind curl, which in turn sustains the warm tongue [*Hafner and Xie*, 2003]. The ASI wake triggered by the Hawaiian Islands trails westward for thousands of kilometers. Following *Xie et al.* [2001]'s calculation, high-pass filtering is applied to highlight the signature of the ASI wake in SST and surface winds (Figure 1b). SST anomalies in the ASI wake are greater than 0.1 °C where sea surface winds converge, indicative of a close relationship between them. The response of LWP to the ASI wake is evident (Figure 1). LWP is positively correlated with the high-pass filtered SST in the area of 170-155 °W, 15-25 °N. Both to the south and north of the Hawaii, the SST anomalies are negative where the easterlies are intensified by islands, implying that stronger winds lower SST by increasing surface heat flux.

We use CALIPSO observations along 14 tracks within the dashed box in Figure 2a to investigate the vertical structure of low-level clouds in the ASI wake. Figures 7a and 7d show the averaged meridional transections of LCT frequency, LWP and high-pass filtered SST and atmospheric meridional circulation averaged between 170-160 °W. The SST anomalies reach 0.2 °C in the ASI wake and are positively correlated with LWP (Figure 7d). The CALIPSO LCT frequency elevated in the warm SST band between 18-20 °N (1.8-2.4 km in elevation), collocated with the maximum high-pass filtered LWP. The increase of low-level clouds is directly related to the upward motion situated over the warm waters. The enhanced LCT frequency is associated with shallow cumulus convection, producing enhanced precipitation over the warm waters (not shown). Over the cold waters both to the north and south, downward motion occurs with a reduction in low-level clouds. As shown later, low-level clouds in the downward motion often occurs at night. Low-level clouds are less frequent where the anomalous vertical motion is weak.

4. Day-night differences

CALIPSO observations near cross points of the daytime and nighttime tracks (indicated with the while and black boxes in Figure 2a) are used to investigate the day-night differences of low-level clouds over different regions. In general, the contrast between the island and ocean is evident in the day-night differences in LCT frequency. Low-level clouds are more prevalent at night over the ocean since the cooling effect of longwave radiation at the cloud top favors the low-level cloud formation, while the daytime solar radiation burns clouds (Figure 8). This day-night difference over the ocean is consistent with the observational results of *Caldwell et al.*, [2005]. Over the Big Island, by contrast, the frequency of LCTs increases from 2% during the nighttime to 5% during the daytime. The altitude of LCT is much higher during the daytime (Figure 8b), indicative of the importance daytime island heating. The probability density functions of low-level cloud fraction (not shown) suggest that the day-night difference over the island is significant. The day-night difference in LCT frequency is stronger in the upstream environment than in the mechanical and ASI wakes.

Figures 7b and 7c show the meridional transections of LCT frequency and meridional circulations within the ASI wake during the daytime and nighttime, respectively. The peak of LCT frequency over the warm waters between 18-20 °N persists the day and night, but the frequent low-level clouds over the cold water only occur during the nighttime. The SST-induced upward motion supports cloud formation even during the day when cloud dissipates in the ambient. It is noted that CALIPSO might miss some low-level clouds in the day due to the daytime solar background noise, which would lower the daytime LCT frequency [*Kacenelenbogen et al.*, 2011].

Vertical motion affects the occurrence and top of low-level clouds. It was considered that enhanced subsidence causes stronger inversion capping MABL, which favors the occurrence of low-level clouds [*Clement et al.*, 2009]. While a more recent work shows that the independent effect of subsidence is to reduce cloud thickness, LWP, and cloud fraction by pushing down the MABL top [*Myers and Norris*, 2013]. Our results indicate that the response of low-level clouds to the downward motion exhibits strong diurnal cycle. In the region with anomalous subsidence, the daytime occurrence of low-level clouds is less frequent, consistent with *Myers and Norris* [2013], while it is much more frequent during the nighttime.

5. Sensitivity to trade wind inversion height

The TWI in the subtropics is caused by the interaction between large-scale subsiding air from the upper troposphere and convection from the sea surface [*Riehl*, 1979]. TWI strongly influences the vertical development of low-level clouds [*Myers and Norris*, 2013] and favors the formation of stratocumulus clouds [*Wood*, 2012]. Sounding data at Lihue on Kauai and Hilo on the Big Island are used to determine the background TWI height following the algorithm of *Cao et al.* [2007]. The LCT frequencies along CALIPSO tracks are composited according to the TWI height (Figure 9). The composite threshold is the mean TWI height (2.3 km) based on Lihue soundings. Lihue station located on the windward coast of Kauai observes the ambient MABL structure (Figure 2b). The background MABL strongly influences the LCT in the open sea where is not disturbed by the islands (Figures 10a and 10b), consistent with *Zhang et al.* [2012]. In the low-TWI height composite along nighttime track N1, LCTs are confined below 2.0 km and the LCT frequency reaches its maximum between 1.5 and 2.0 km (Figure 9b). In the high-TWI height composite, on the other hand, considerable LCTs penetrate above 2.3 km and the LCT frequency peaks near 2.5 km (Figure 9a). The daytime relationship between LCT along track D1 and TWI height is similar (not shown).

In the low-TWI height composite, the most LCTs over Kauai are beneath the 2.3 km (Figure 9c), indicating a strong capping effect of the background TWI. The maximum LCT frequency at the peak altitude exceeds 10%. In the composite with TWI higher than 2.3 km (Figure 9e), low-level clouds develop much higher than the low-TWI height composite and LCTs are prevalent between 1.2 and 2.5 km. Thus, the large-scale circulation exerts a strong influence on the vertical development of low-level clouds over the Hawaiian Islands by altering the background TWI height.

The LCT sensitivity of the over the Big Island (Figures 9e and 9f) generally resembles that over Kauai. LCTs are lower with lower TWI at Hilo, and higher LCTs with higher TWI. It is interesting that the LCTs between 19.2-19.8 °N over the island along track D2 are not very sensitive to background TWI height, and that the LCTs are much higher than 2.3 km in the low-TWI height composite (Figure 9f). All this indicates that the background TWI and the daytime surface heating dominate the atmospheric boundary layer structure over the islands.

The distance between cloud top and island surface is much smaller in the low-TWI than the high-TWI height composite (Figures 9e and 9f), indicative of more frequent occurrence of mountain fog. This supports the argument of *Juvik and Ekern* [1978] that TWI influences the ecosystem of the Big Island by modifying mountain fog and rainfall.

Figure 10 clarifies the relationship between heights of TWI and maximum LCTs over different regions. Both LCTs over the windward slope of Kauai and in the upstream environment are highly correlated with Lihue TWI height with correlation coefficients above 99% confidence level (Figure 10a), suggesting the strong control of LCT by TWI height. The correlation coefficient for Kauai windward slope LCT is higher than the value for upstream LCT, possibly due to the shorter distance between the Kauai windward slope and Lihue station. LCT observations along track D2 near the Big Island are separated into the north slope, central mountain, and south slope regions (Figure 10b), as indicated by blue, black and red lines in Figure 9e. The correlation between LCT and Hilo TWI is high over the north and south slopes, but is low in the central region because of daytime convection.

6. Summary and discussion

During boreal summer, steady northeasterly trade winds impinge on the Hawaiian Islands producing wakes of multi-spatial scales from tens to thousands kilometers. We have investigated the vertical structure of low-level clouds over the islands and in their wakes using CALIPSO, other high-resolution satellite observations, the ERA-Interim reanalysis and atmospheric soundings at Lihue and Hilo. Our results reveal that the vertical structure of low-level clouds shows evident effects of the Hawaiian Islands.

LCT frequency observed by CALIPSO is almost featureless in the upstream of the Hawaiian Islands where the trade winds are not disturbed by the islands. The influence of orographic lifting by the Kauai upslope flow is pronounced in the vertical structure of low-level clouds. The vertically integrated LCT frequency over the windward slope of Kauai exceeding 80 % while it decreases sharply to lower than 20 % over the north and south waters off Kauai, a value even less than the upstream environment (~30 %). The vertical structure over Oahu windward slope is similar to Kauai, but the response is weaker due to the lower elevation of the island.

In the nighttime near-island wake, CALIPSO captures a striking "cloud hole" below 1.6 km in the lee of Kauai. It supports the *Yang et al.* [2008b]'s argument that the cold advection from Kauai at night increases the SLP and lower the low-level cloud frequency. This effect is valid only below the level of the cold advection above which the low-level clouds are not influenced by the island.

Over the Big Island, CALIPSO tracks cover the leeside slope of the Big Island south of 20 °N. The daytime vertical structure of LCT frequency features three maxima, separated by Mauna Loa and Mauna Kea. These three peaks are caused by orographic lifting of the combined westerly return flow and anabatic wind, often stand above than the background TWI, indicative of the effects of daytime surface heating and convection. CALIPSO observes the clouds over the windward slope and over the leeside sea of Kohala Mountains (~20 °N) along track N1 and D2 respectively, and captures a steep transition from high frequent LCT to much low frequent LCT (Figures 5e and 5f).

Two elongated counterrotating quasi-steady eddies form behind the Big Island due to mechanical effects of the island. LCT frequency reaches its maximum over the cyclonic eddy, consistent with the TMI LWP and QuikSCAT surface winds. In the far-field ASI wake, LCT frequency peaks with the anomalous ascent motion over the warm SST band while low-level clouds are less prevalent where the vertical motion is weak.

Finally, we have studied the effects of background TWI height on the vertical development of low-level clouds over the islands. It is found that the background TWI height exerts strong influence on LCTs over Kauai. The height of LCT maximum is highly and positively correlated with the concurrent background TWI height. Over the Big Island, the correlation is relatively low between LCTs and the TWI height at Hilo because of daytime convection.

On the Big Island, the distance between LCT and the surface is less than 250 m (Figures 5e and 5f), indicating that some clouds touch island surface forming mountain fogs. *Juvik and Ekern* [1978] reported the mountain fog on leeward of Mauna Loa increases with elevation up to at least 2000 m, consistent with our results using CALIPSO (Figure 5e). Similarly, *Giambelluca and Nullet* [1991] found a fog zone between 1200 m and 1800 m over the slopes of Haleakala. The fog catchment in the fog zone on the Big Island is a major component of the water balance, and therefore may have significant ecological impacts [*Juvik and Ekern*, 1978]. This study offers new insights into the thermal and mechanical effects of the Hawaiian Islands on the vertical structure of cloud. The results imply that the background TWI height has significant ecological impact by affecting the mountain fog occurrence.

Acknowledgments.

The data in this study are obtained from the atmospheric scientific data center of NASA (CALIPSO; http://www-calipso.larc.nasa.gov/), Remote Sensing System (QuikSCAT, TMI LWP; http://www.remss.com/), the ECMWF data sever (ERA-Interim; http://apps.ecmwf.int/datasets/), National Climate Data Center of NOAA (AVHRR SST; http://www.ncdc.noaa.gov/sst/), and University of Wyoming (atmospheric soundings; http://weather.uwyo.edu/upperair/sounding.html). This study was conducted while J.-W. Liu was a visiting student at Scripps. This work is supported by the National Basic Research Program of China (2012CB955602), and the Natural Science Foundation of China (41175006, 41275049). S.P.X. acknowledges NASA support.

Reference

Bony, S., and J.-L. Dufresne (2005), Marine boundary layer clouds at the heart of tropical cloud feedback uncertainties in climate models, *Geophys. Res. Lett.*, *32*(20), L20806, doi:10.1029/2005GL023851, doi:10.1029/2005GL023851.

Bouniol, D., F. Couvreux, P.-H. Kamsu-Tamo, M. Leplay, F. Guichard, F. Favot, and E. J. O'Connor (2012), Diurnal and seasonal cycles of cloud occurrences, types, and radiative impact over West Africa, *J. Appl. Meteorol. Climatol.*, *51*(3), 534–553, doi:10.1175/JAMC-D-11-051.1.

Caldwell, P., C. S. Bretherton, and R. Wood (2005), Mixed-layer budget analysis of the diurnal cycle of entrainment in southeast Pacific stratocumulus., *J. Atmos. Sci.*, *62*, 3775–3791.

Cao, G., T. W. Giambelluca, D. E. Stevens, and T. a. Schroeder (2007), Inversion variability in the Hawaiian trade wind regime, *J. Clim.*, *20*(7), 1145–1160, doi:10.1175/JCLI4033.1.

Clement, A. C., R. Burgman, and J. R. Norris (2009), Observational and model evidence for positive low-level cloud feedback., *Science (80-.).*, *325*(5939), 460–464, doi:10.1126/science.1171255.

Dee, D. P. et al. (2011), The ERA-Interim reanalysis: configuration and performance of the data assimilation system, *Q. J. R. Meteorol. Soc.*, *137*(656), 553–597, doi:10.1002/qj.828.

Giambelluca, T., and D. Nullet (1991), Influence of the trade-wind inversion on the climate of a leeward mountain slope in Hawaii, *Clim. Res.*, *1*, 207–216.

Hafner, J., and S.-P. Xie (2003), Far-field simulation of the Hawaiian wake: Sea surface temperature and orographic effects, *J. Atmos. Sci.*, *60*, 3021–3032.

Hartmann, D. L., M. E. Ockert-Bell, and M. L. Michelsen (1992), The effect of cloud type on Earth's energy balance: Global analysis, *J. Clim.*, *5*(11), 1281–1304.

Hilburn, K. A., and F. J. Wentz (2008), Intercalibrated passive microwave rain products from the unified microwave ocean retrieval algorithm (UMORA), *J. Appl. Meteorol. Climatol.*, *47*(3), 778–794.

Juvik, J. O., and P. C. Ekern (1978), A climatology of mountain fog on Mauna Loa, Hawaii Island, *Tech. Rep. 118. 63 pp.*, Water Resour. Res. Cent. Univ. of Hawaii at Manoa, Honolulu.

Kacenelenbogen, M., M. a. Vaughan, J. Redemann, R. M. Hoff, R. R. Rogers, R. a. Ferrare, P. B. Russell, C. a. Hostetler, J. W. Hair, and B. N. Holben (2011), An accuracy assessment of the CALIOP/CALIPSO version 2/version 3 daytime aerosol extinction product based on a detailed multi-sensor, multi-platform case study, *Atmos. Chem. Phys.*, *11*(8), 3981–4000, doi:10.5194/acp-11-3981-2011.

Liu, J.-W., S.-P. Xie, J. R. Norris, and S.-P. Zhang (2014), Low-level cloud response to the Gulf Stream front in winter using CALIPSO, *J. Clim.*, *27*(12), 4421–4432, doi:10.1175/JCLI-D-13-00469.1.

Medeiros, B., L. Nuijens, C. Antoniazzi, and B. Stevens (2010), Low-latitude boundary layer clouds as seen by CALIPSO, *J. Geophys. Res.*, *115*, D23, doi: 10.1029/2010JD014437.

Myers, T. a., and J. R. Norris (2013), Observational evidence that enhanced subsidence reduces subtropical marine boundary layer cloudiness, *J. Clim.*, *26*(19), 7507–7524, doi:10.1175/JCLI-D-12-00736.1.

Norris, J. R. (1998a), Low cloud type over the ocean from surface observations. Part I: Relationship to surface meteorology and the vertical distribution of temperature and moisture, *J. Clim.*, *11*, 369–382.

Norris, J. R. (1998b), Low cloud type over the ocean from surface observations. Part II: Geographical and seasonal variations, *J. Clim.*, *11*, 383–403.

Reynolds, R. W., T. M. Smith, C. Liu, D. B. Chelton, K. S. Casey, and M. G. Schlax (2007), Daily high-resolution-blended analyses for sea surface temperature, *J. Clim.*, *20*(22), 5473–5496, doi:10.1175/2007JCLI1824.1.

Riehl, H. (1979), *Climate and Weather in the Tropics.*, Academic Press, 623pp.

Schroeder, T. A. (1993), Climate controls, *Prevail. trade Wind*, M. Sanderson, Ed., University of Hawaii Press, 12–36.

Sherwood, S. C., S. Bony, and J.-L. Dufresne (2014), Spread in model climate sensitivity traced to atmospheric convective mixing., *Nature*, *505*(7481), 37–42, doi:10.1038/nature12829.

Smith, R., and V. Grubišic (1993), Aerial observations of Hawaii's wake, *J. Atmos. Sci.*, *50*(22), 3728–3750.

Stein, T. H. M., D. J. Parker, J. Delanoë, N. S. Dixon, R. J. Hogan, P. Knippertz, R. I. Maidment, and J. H. Marsham (2011), The vertical cloud structure of the West

African monsoon: A 4 year climatology using CloudSat and CALIPSO, *J. Geophys. Res.*, *116*(D22), D22, 10.1029/2011JD016029.

Vaughan, M. a., K. a. Powell, D. M. Winker, C. a. Hostetler, R. E. Kuehn, W. H. Hunt, B. J. Getzewich, S. a. Young, Z. Liu, and M. J. McGill (2009), Fully automated detection of cloud and aerosol layers in the CALIPSO lidar measurements, *J. Atmos. Ocean. Technol.*, *26*(10), 2034–2050, doi:10.1175/2009JTECHA1228.1.

Winker, D. M., M. A. Vaughan, A. Omar, Y. Hu, K. A. Powell, Z. Liu, W. H. Hunt, and S. A. Young (2009), Overview of the CALIPSO mission and CALIOP data processing algorithms, *J. Atmos. Ocean. Technol.*, *26*(11), 2310–2323.

Wood, R. (2012), Stratocumulus clouds, *Mon. Weather Rev.*, *140*(8), 2373–2423, doi:10.1175/MWR-D-11-00121.1.

Xie, S. P., W. T. Liu, Q. Liu, and M. Nonaka (2001), Far-reaching effects of the Hawaiian Islands on the Pacific Ocean-atmosphere system., *Science*, *292*(5524), 2057–60, doi:10.1126/science.1059781.

Yang, Y., and Y. Chen (2003), Circulations and rainfall on the lee side of the island of Hawaii during HaRP., *Mon. Weather Rev.*, (1981), 2525–2542.

Yang, Y., and Y.-L. Chen (2008), Effects of Terrain Heights and Sizes on Island-Scale Circulations and Rainfall for the Island of Hawaii during HaRP, *Mon. Weather Rev.*, *136*(1), 120–146, doi:10.1175/2007MWR1984.1.

Yang, Y., S.-P. Xie, and J. Hafner (2008a), Cloud patterns lee of Hawaii Island: A synthesis of satellite observations and numerical simulation, *J. Geophys. Res.*, *113*(D15), D15126, doi: 10.1029/2008JD009889., doi:10.1029/2008JD009889.

Yang, Y., S.-P. Xie, and J. Hafner (2008b), The thermal wake of Kauai Island: Satellite observations and numerical simulations, *J. Clim.*, *21*(18), 4568–4586, doi:10.1175/2008JCLI1895.1.

Zhang, C., Y. Wang, A. Lauer, K. Hamilton, and F. Xie (2012), Cloud base and top heights in the Hawaiian region determined with satellite and ground-based measurements, *Geophys. Res. Lett.*, *39*, D15, doi: 10.1029/2012GL052355, doi:10.1029/2012GL052355.

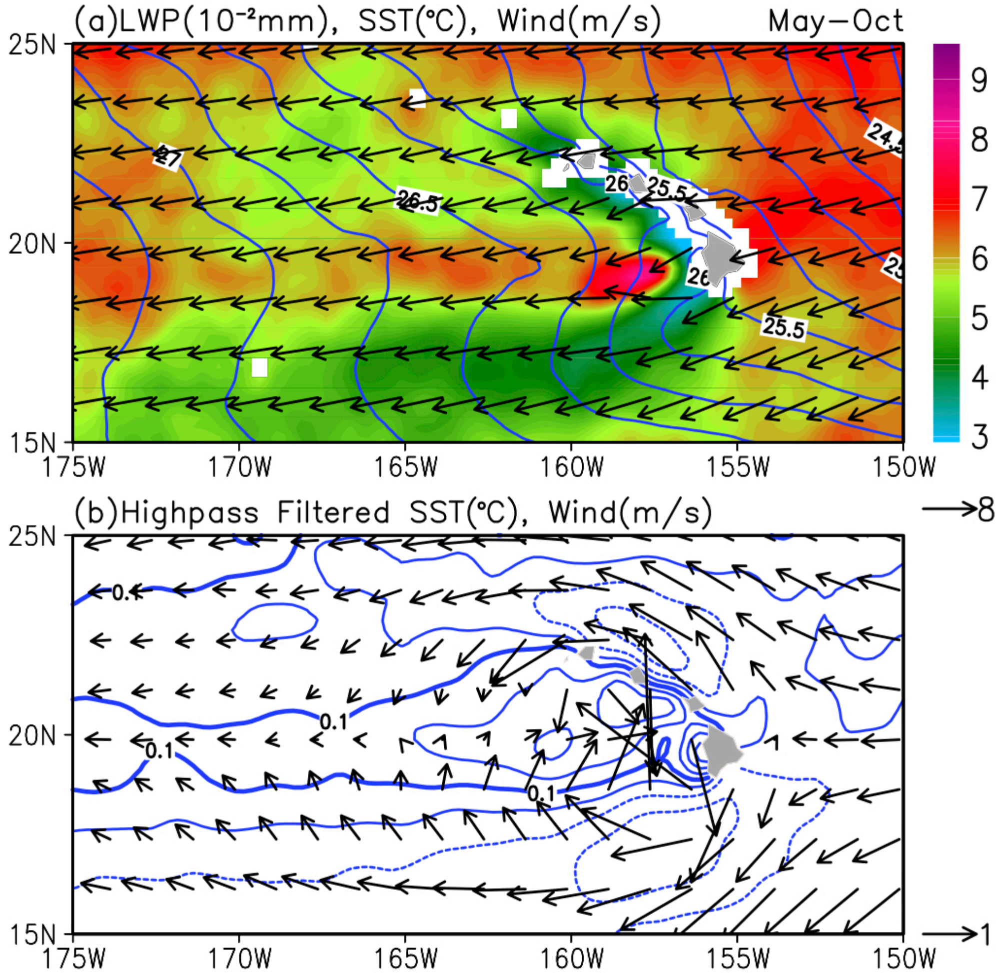

Figure 1. Summer (May to October, the same hereafter) climatology: (a) TMI LWP (shading in 10^{-2} mm), AVHRR SST [contours; contour intervals (CI) = 0.25 °C], and QuikSCAT wind vectors (m s^{-1}); (b) high-pass filtered SST (contours; CI = 0.1 °C) and surface winds (vectors; m s^{-1}) by subtracting an 8° moving average following *Xie et al.* [2001].

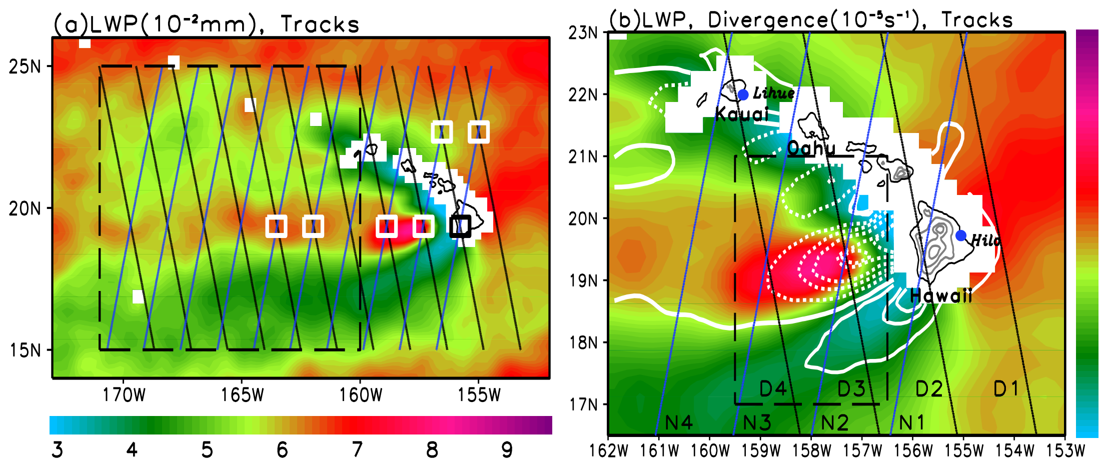

Figure 2. Summer LWP climatology (color shading in 10^{-2} mm) and CALIPSO tracks (lines). The black and blue lines denote CALIPSO tracks during the daytime (around 14:00 HST) and nighttime (around 02:00 HST), respectively. The daytime and nighttime CALIPSO tracks are numbered with D1-4 and N1-4 in (b), respectively. The contours in (b) are surface wind divergence (solid contours indicate zero and positive values, and dashed indicate negative; CI = 10^{-5} s^{-1}) from QuikSCAT. The grey contours indicate the topography of the Hawaiian Islands (CI = 500 m) in (b), and the blue dots denote Hilo and Lihue stations. The dashed line box in (a) represents the domain of the ASI wake. The CALIPSO observations within the white and black boxes in (a) are used to investigate the day-night differences of low-level clouds.

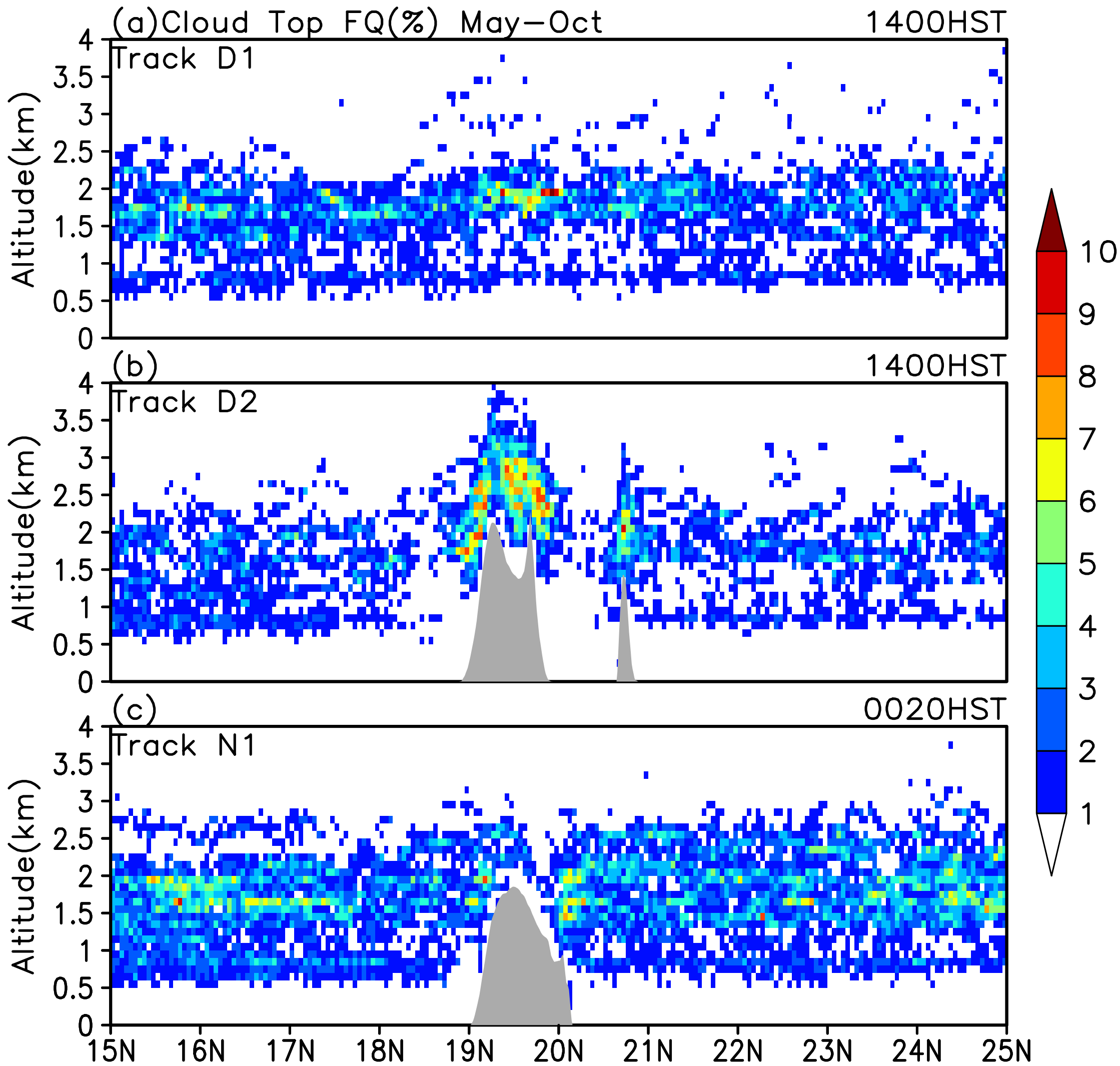

Figure 3. LCT frequencies (color filled grid; %) in summer along tracks D1 (a), D2 (b) and N1 (c). The grey shades denote the island topography along CALIPSO tracks.

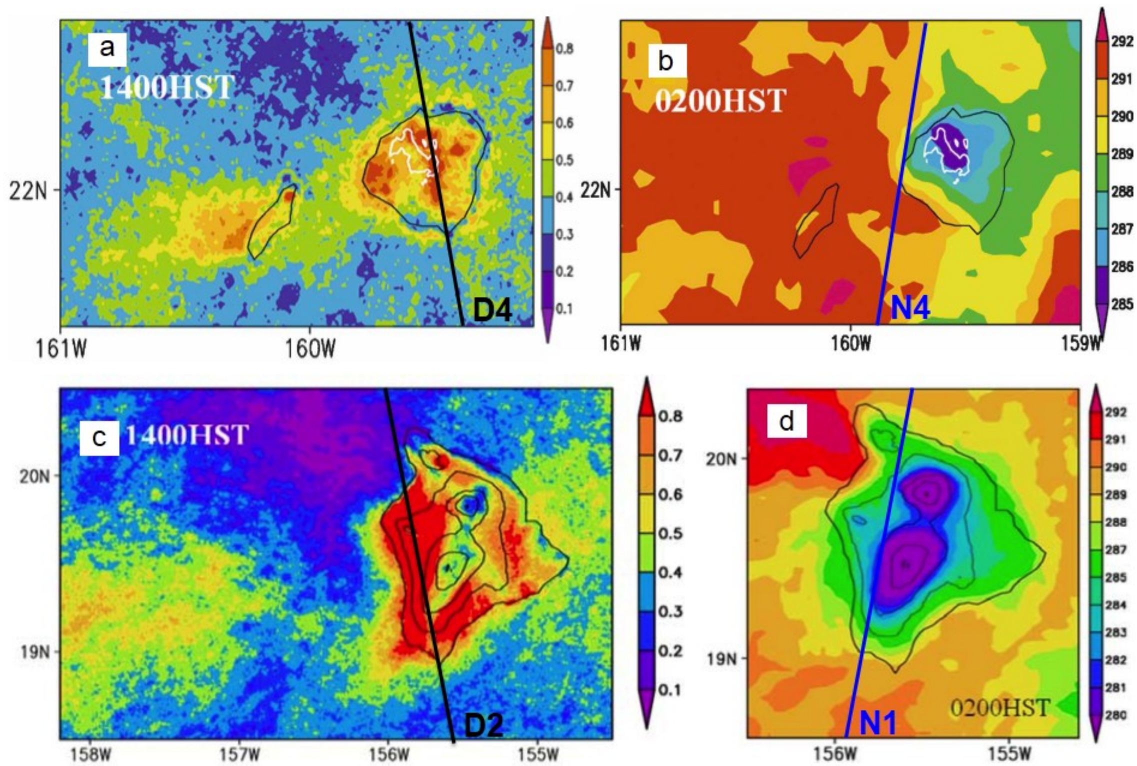

Figure 4. Cloud frequency during June-August 2004-05 near Kauai (a) and the Big Island (c) at 1400 HST based upon MODIS Aqua. Brightness temperature (K) at 0200 HST during August 2005 derived from the GOES-10 IR channel 5 (b, d). The black and blue lines indicate the CALIPSO tracks whose reference numbers are consistent with in Figure 2b. Adapted from *Yang et al.* [2008a, 2008b] by permission of the American Meteorological Society.

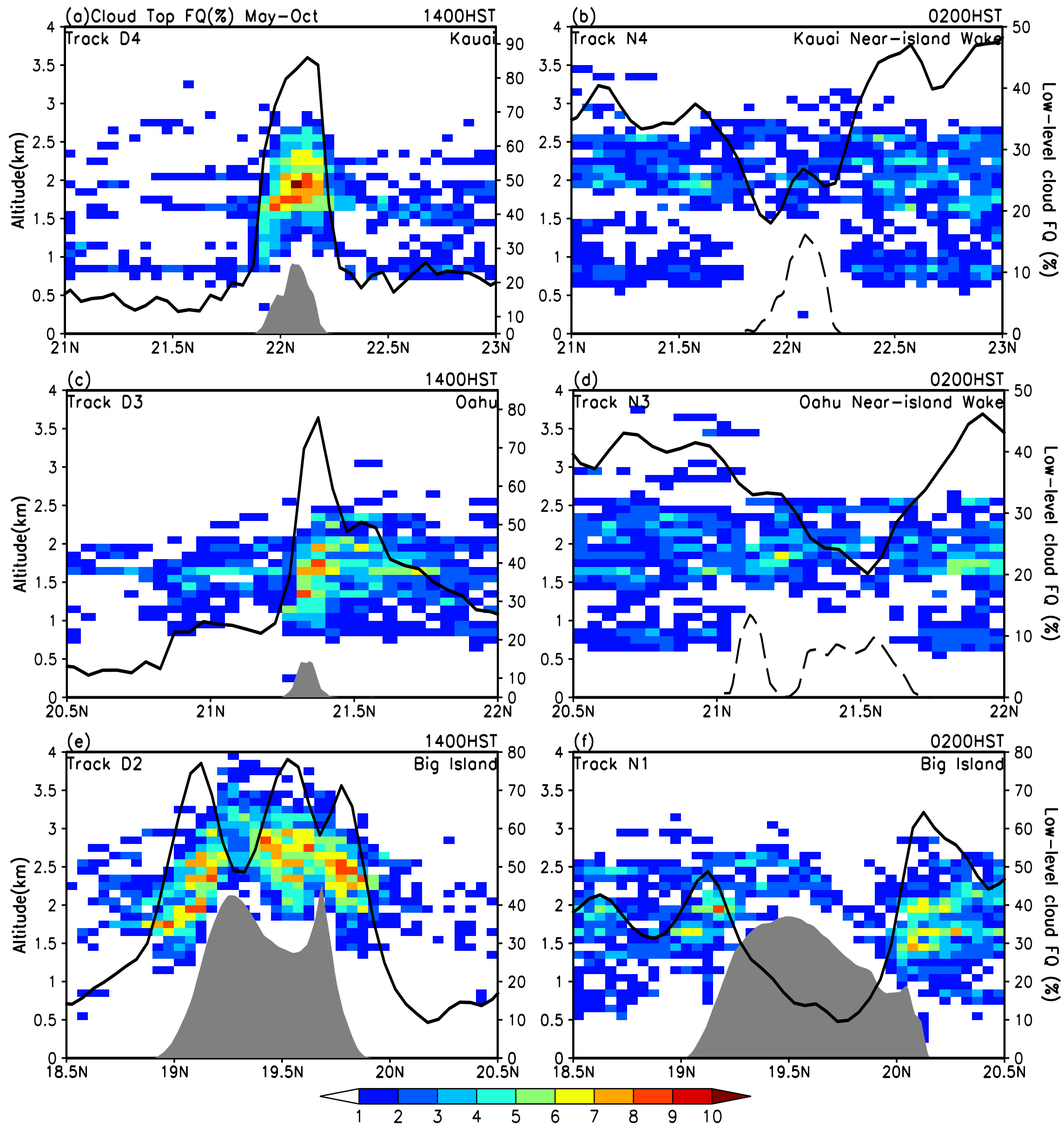

Figure 5. LCT frequencies (filled grid; %) along tracks D4 (a), N4 (b), D3 (c), N3 (d), D2 (e), and N1 (f). The grey shades in (a, c, e, f) denote the island topography along CALIPSO tracks. The dashed lines in (b) and (d) are the zonal maximum topography of the islands of Kauai, Oahu and Molokai. The black lines are vertically integrated LCT frequency.

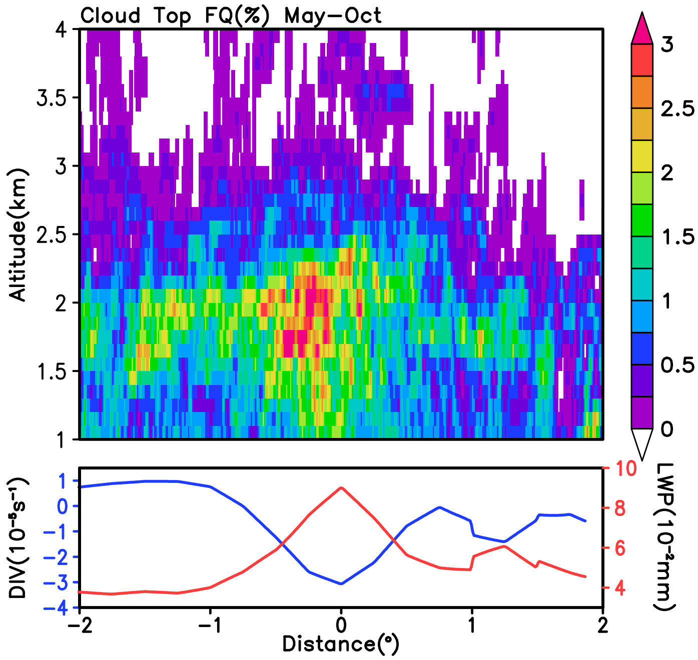

Figure 6. The meridional transections of LCT frequency (filled grid; %), QuikSCAT divergence (blue line; 10^{-5} s^{-1}) and TMI LWP (red line; 10^{-2} mm). The transections are composited referenced to the maximum LWP along CALIPSO tracks between 17°N and 21 °N and derived from variables along tracks N2, N3, D3 and D4; distance to the maximum SLP is in degree latitude with negative denoting to the south and positive to the north. The LCTs over island are omitted.

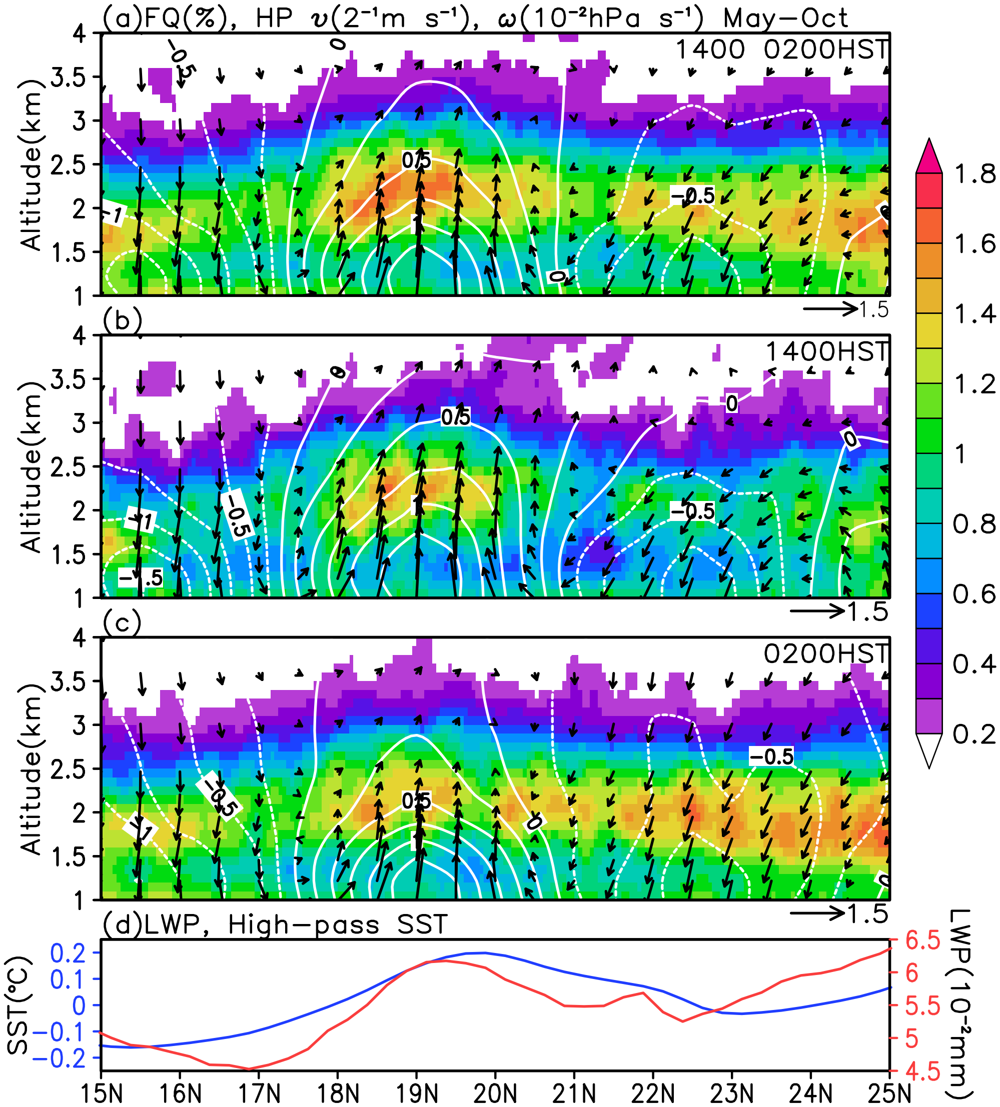

Figure 7. Meridional transections of LCT frequency (filled grid; %), ERA-Interim upward velocity (contours; CI = 0.25×10^{-2} hPa) and meridional winds (vectors; 2^{-1} m s^{-1}) for the day-night mean (a), daytime (b) and nighttime (c), respectively. (d) Day-night averaged meridional transections high-pass filtered AVHRR SST (blue line; °C), and TMI LWP (red line; 10^{-2} mm). The meridional transections are derived by zonally averaging within the dashed box in Figure 2a.

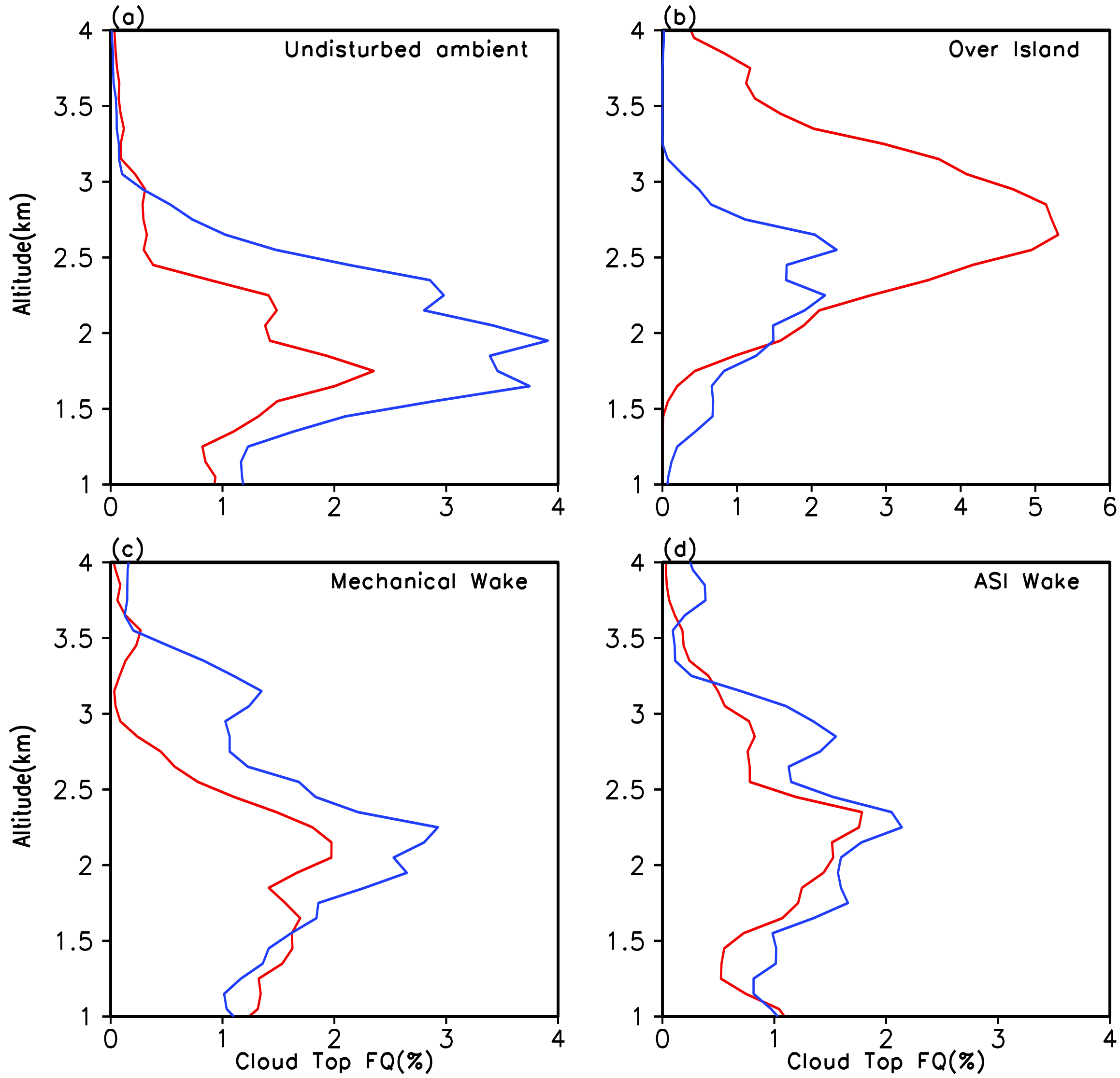

Figure 8. Profiles of LCT frequency (%) during the daytime (14:00 HST, red lines) and the nighttime (02:00 HST, blue lines) in the undisturbed environment (a), over Big Island (b), in the mechanical wake (c) and in the ASI wake (d). The frequency profiles are averaged within 0.4° meridional bins centered on the cross points between tracks (D1 and N1, D2 and N2), (D2 and N1), (D3 and N2, D4 and N3), which are indicated with boxes in Figure 2a for (a-d), respectively.

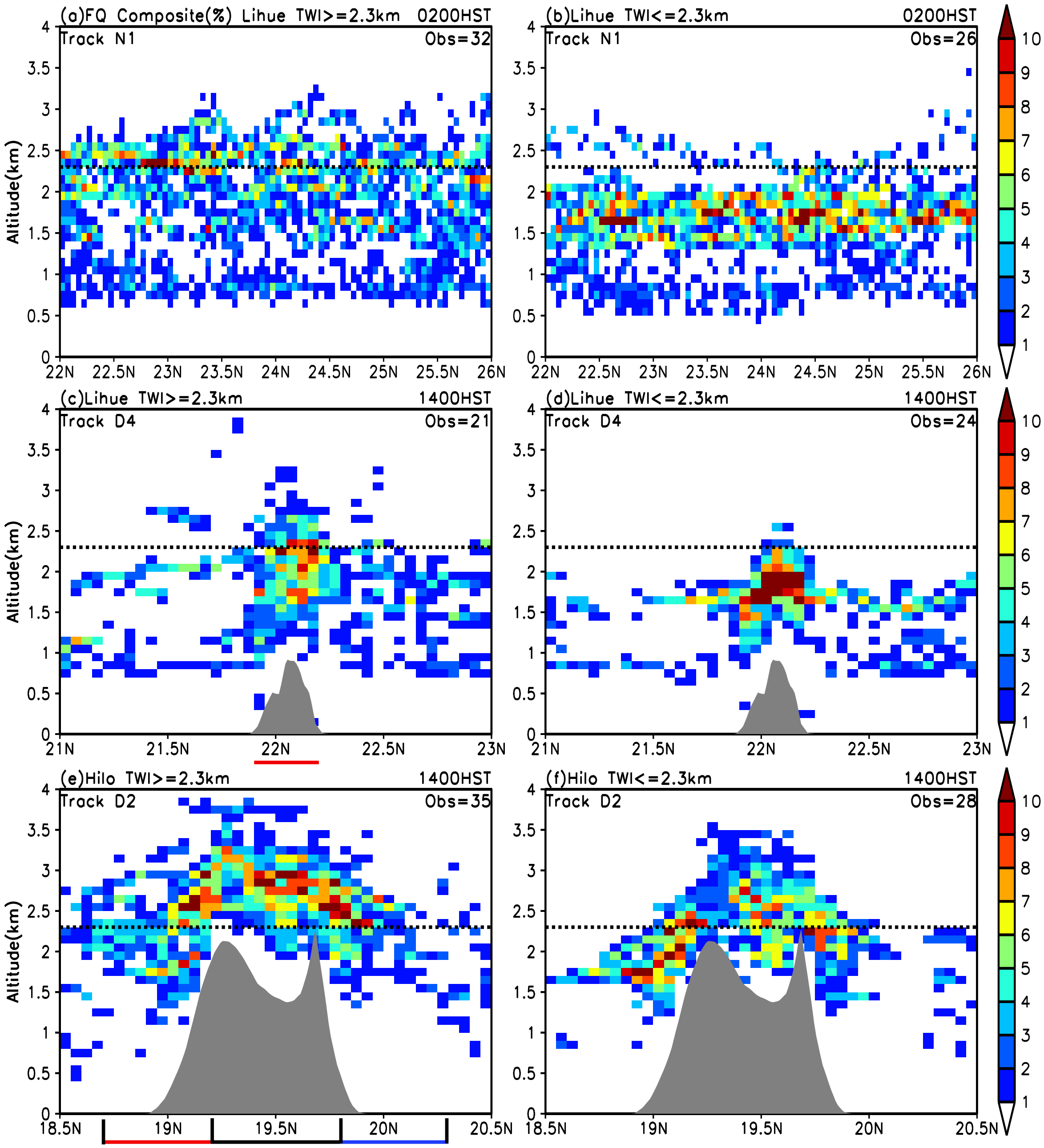

Figure 9. The composite LCT frequencies (filled grid; %) along track N1, D4, and D2 with TWI higher than 2.3 km (a, c, e), and with TWI lower than 2.3 km (b, d, f). The dashed lines indicate the threshold of TWI height, which is the mean TWI height based from Lihue soundings. The grey shades denote the topography along CALIPSO tracks. TWI height is calculated following the algorithm of *Cao et al.* [2007] using soundings at Lihue for (a-d), and at Hilo for (e, f). The red line beneath (e) indicates the region in which TWI height maxima are picked for the red scatters in Figure 10a, and the red, black and blue lines are for the red, black and blue scatters in Figure 10b.

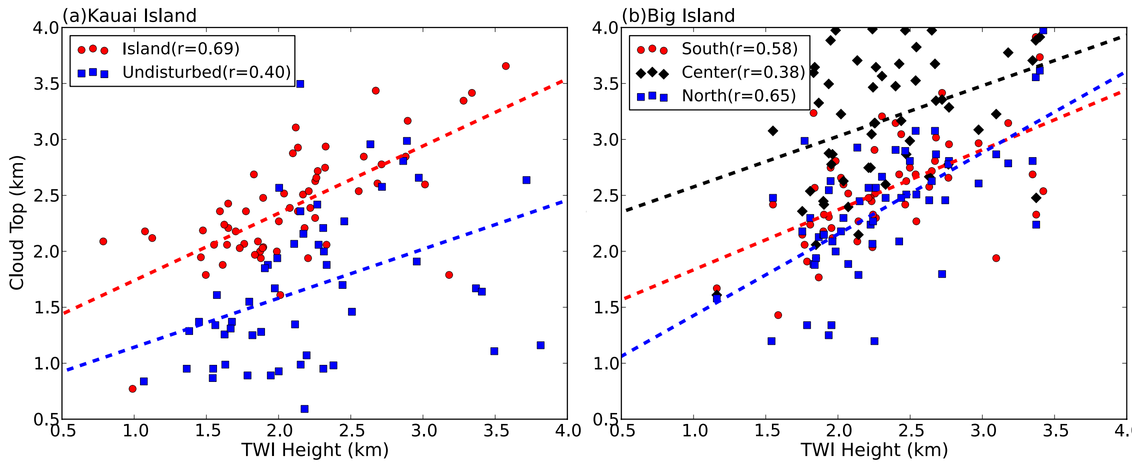

Figure 10. Scatter diagrams of background TWI height and the maximal cloud top. (a) TWI height is calculated using soundings at Lihue, and the cloud top is the maximal cloud top between 21.9-22.2°N along tracks N2 and N4 for blue and red markers, respectively. (b) TWI height is derived from soundings at Hilo, and the maximal cloud tops for the red, black, and blue scatters are picked along track D2 between 18.7-19.2 °N (south slope), 19.2-19.8 °N (central mountain), and 19.8-20.3 °N (north slope). The regions in (a) and (b) are indicated with color lines in Figures 10c and 10e, respectively.